Supporting Information

New Rofecoxib-Based Mechanochromic Luminescencent Materials and Investigations on Their Aggregation-Induced Emission, Acidochromism, and LD-Specific Bioimaging

Liwei Chen [a, #], Renfu Li [b, #], Xinli Wang [c, #], Zexin Wang [a], Xiang Lin [a], Lu Yang [a], Yunpeng Yao [b], Shitao Sun [d], Zhenli Li [d], Jinle Hao [d], Bin Lin [d], Xueyuan Chen [b, *] and Lijun Xie [a, *]

[a] Fujian Provincial Key Laboratory of Screening for Novel Microbial Products, Fujian Institute of Microbiology, Fuzhou, Fujian 350007, PR China

[b] CAS Key Laboratory of Design and Assembly of Functional Nanostructures, and Fujian Key Laboratory of Nanomaterials, Fujian Institute of Research on the Structure of Matter, Chinese Academy of Sciences, Fuzhou, Fujian 350002, PR China

[c] Department of Medical Oncology, Fujian Medical University Union Hospital, Fuzhou, Fujian 350007, P.R. China

[c] Department of Medicinal Chemistry, School of Pharmaceutical Engineering, Shenyang Pharmaceutical University, Shenyang, Liaoning 110016, P.R. China

Author contribution

*Corresponding author

Email address: lijunxie8224@outlook.com (L.X.) or xchen@fjirsm.ac.cn (X.C.)

[#]Equal contribution

Table of Contents

1. Experimental details.

Cell Culture and Fluorescence Imaging

Cell culture: Human cervical cancer (HeLa) cell lines were obtained from American type culture collection. HeLa cells utilized in the experiments were cultured in Dulbecco's modified Eagle's medium (DMEM) supplemented with 10% fetal bovine serum (FBS) and then incubated at 37℃ in an atmosphere of 5% CO_2. The cells were washed with ice-cold PBS three times and then incubated with PBS-free fresh media.

Fluorescence Imaging: We assessed the ability of **Y7** in different cell lines. **Y7** was incubated with carcinoma cell lines HeLa for 0.5 h, and they washed with PBS buffer 3 times. Subsequently, the fluorescence images were taken. Cell imaging showed that the fluorescence intensity of the HeLa cells increased after treatment with **Y7**.

2. The structure of 2a1.

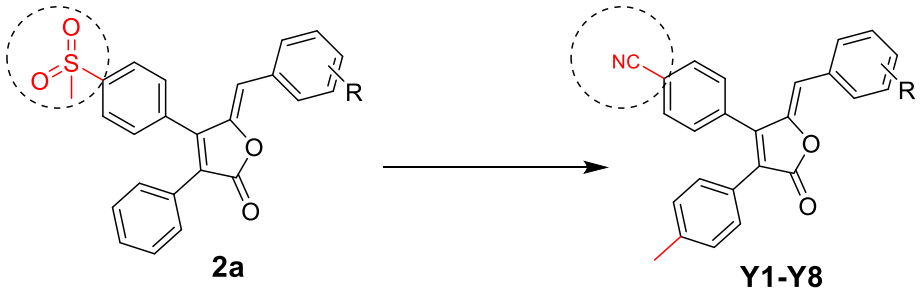

Scheme S1. The synthetic route and structure of **2a1**.

3. The absorbance spectra of compounds in DMSO solvent.

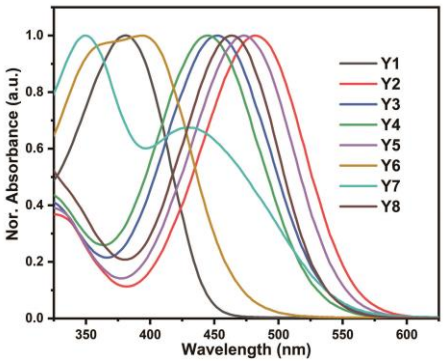

Figure S1. Normalized absorption spectra of **Y1-Y8 (**50 μM**)** in DMSO solution.

Table S1. Maximum absorbance and emission of compounds in DMSO.

compounds	λ_{abs}(nm)[a]	λ_{em}(nm)[b]
Y1	382	526
Y2	482	648
Y3	464	650
Y4	446	656
Y5	474	658
Y6	372	668
Y7	350	670
Y8	464	694

a: maximum absorbance wavelength; b: maximum emission wavelength

4. Beer-Lambert's plot and linear fitting of compounds.

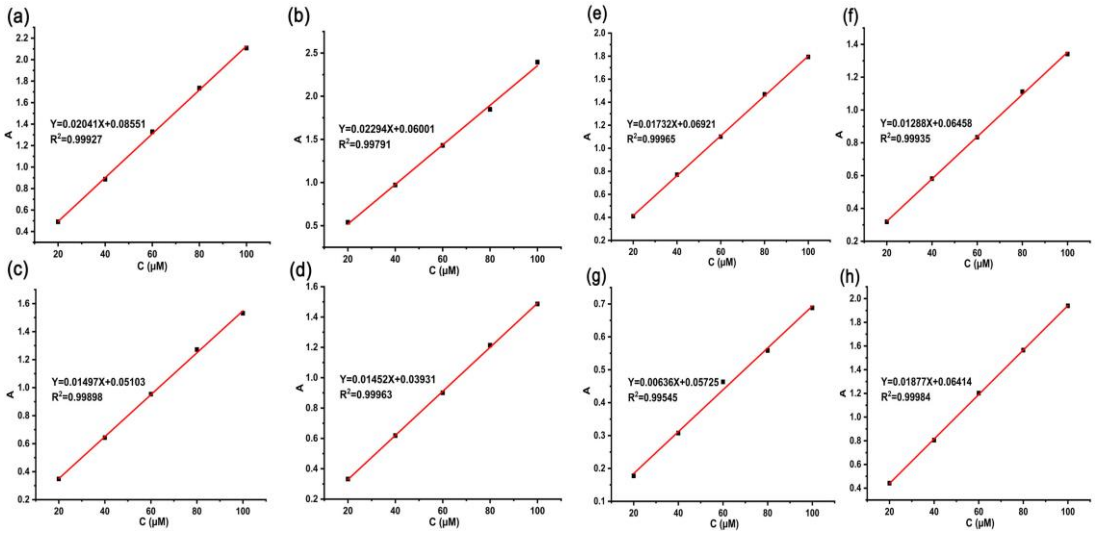

Figure S2. Beer-Lambert's plot and linear fitting of **Y1** (a), **Y2** (b), **Y3** (c), **Y4** (d), **Y5**(e), **Y6** (f), **Y7** (g) and **Y8** (h). (Y= 0.02041X+0.08551, R^2= 0.99927; Y= 0.02294X+0.06001, R^2= 0.99791; Y= 0.01497X+0.05103, R^2= 0.99898; Y= 0.01452X+0.03931, R^2= 0.99963; Y= 0.01732X+0.06921, R^2= 0.99965; Y= 0.01288X+0.06458, R^2= 0.99935; Y= 0.00636X+0.05725, R^2= 0.99545; Y= 0.01877X+0.06414, R^2= 0.99984.)

5. UV-vis absorption spectra and photo-physical date of compounds in different solvents.

5.1 The absorption spectra of Y6.

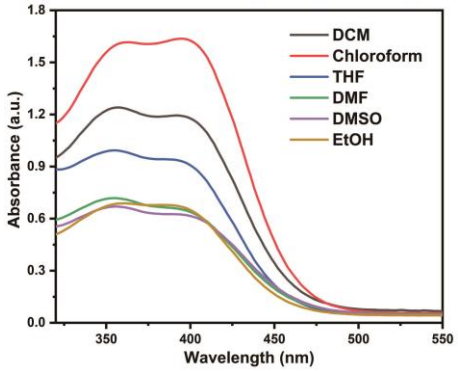

Figure S3. The absorption of **Y6** (5×10^{-5} mol/L) in different solvents.

5.2 The absorption spectra of Y7.

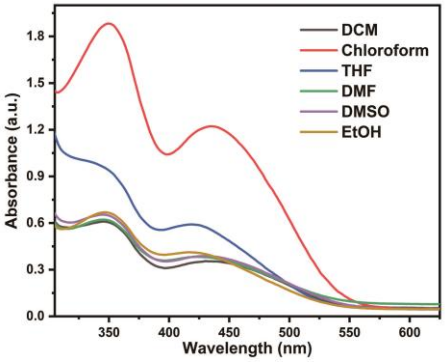

Figure S4. The UV-vis absorption spectra of **Y7** (5×10^{-5} mol/L**)** in different solvents.

5.3 The absorption spectra of Y8.

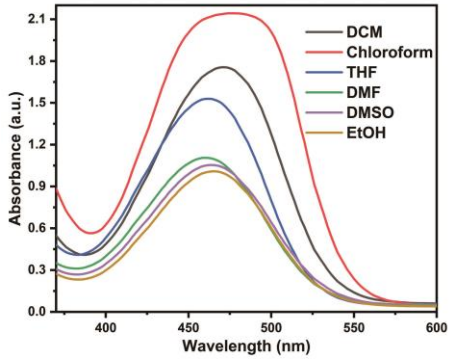

Figure S5. The UV-vis absorption spectra of **Y8** (5×10^{-5} mol/L) in different solvents.

5.4 The photo-physical data of compounds in different solvents.

Table S2. The photo-physical data of **Y6**, **Y7** and **Y8** in different solvents.

Compounds	Solvent	λ_{abs}(nm)[a]	λ_{em}(nm)[b]	Stokes shifts(nm)	$\Delta v(cm^{-1})$[d]
Y6	Chloroform	362	606	244	11122
	THF	354	626	272	12274
	DCM	358	648	290	12500
	EtOH	360	644	284	12250
	DMF	354	660	306	13097
	DMSO	356	674	318	13253
Y7	Chloroform	350	634	284	12798
	THF	350	638	288	12897
	DCM	346	630	284	13028
	EtOH	348	646	298	13255
	DMF	346	664	318	13841
	DMSO	346	672	326	14020
Y8	Chloroform	476	632	156	5185
	THF	470	640	170	5651
	DCM	472	650	178	5801
	EtOH	466	658	186	6261
	DMF	462	674	212	6808
	DMSO	464	698	234	7225

[a] Maximum absorption; [b] Maximum emission; [c] Stokes shifts; [d] Δv, were calculated using the equation $1/\lambda_{abs}$-$1/\lambda_{em}$.

6. Photoluminescence quantum yield of Y7.

Table S3.The photoluminescence quantum yield of **Y7** in DMSO solution of 50 μM.

compound	quantum yield
(0% H_2O) **Y7**	0.1%
(60% H_2O) **Y7**	12.5%

7. PL spectra of Y2 and Y4 in DMSO-water mixtures.

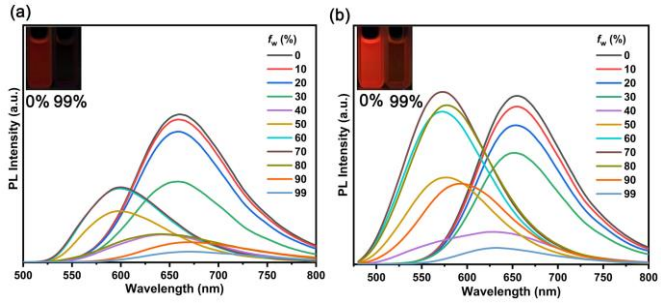

Figure S6. The PL spectra of **Y2** (a) and **Y4** (b) with different f_w in DMSO (25 μM). Inset: the photographs of **Y2** (a), and **Y4** (b) in 0% water and 99% water were taken under a 365 nm with hand-held UV lamp.

8. AIE property of Y6, Y7 and Y8.

8.1 AIE property of Y6.

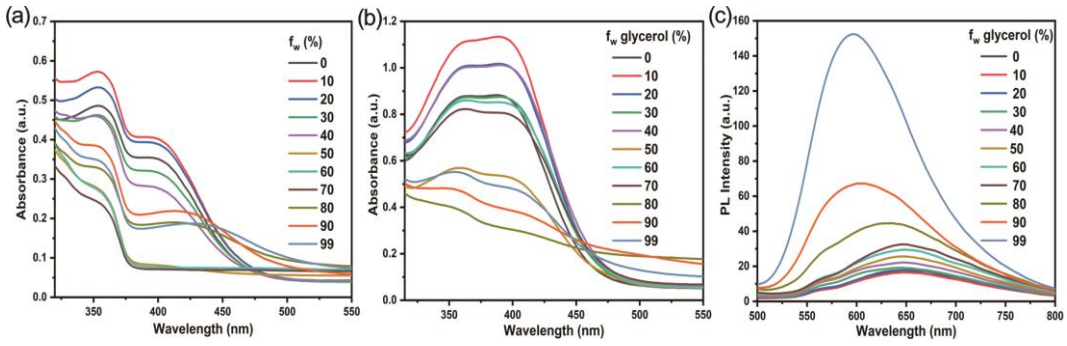

Figure S7. The absorption spectra of **Y6** in different proportions of water and DMSO (a). The absorption (b) and emission spectra (c) of **Y6** in different proportions of glycerol and ethanol.

8.2 AIE property of Y7.

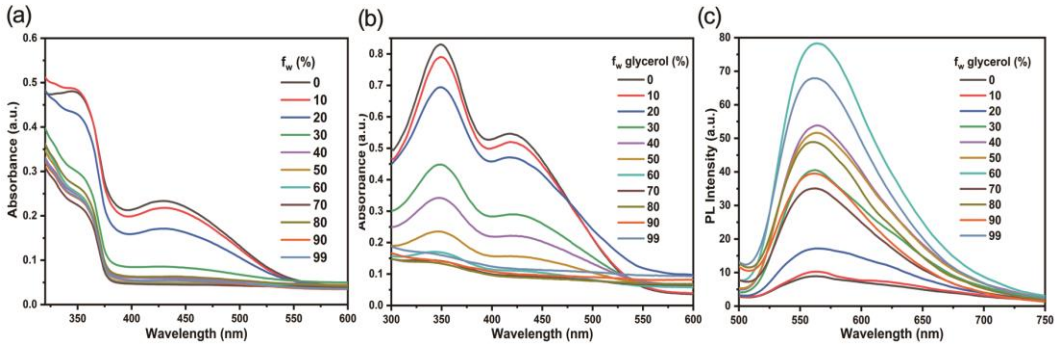

Figure S8. The absorption spectra of **Y7** in different proportions of water and DMSO (a). The absorption (b) and emission spectra (c) of **Y7** in different proportions of glycerol and ethanol.

8.3 AIE property of Y8.

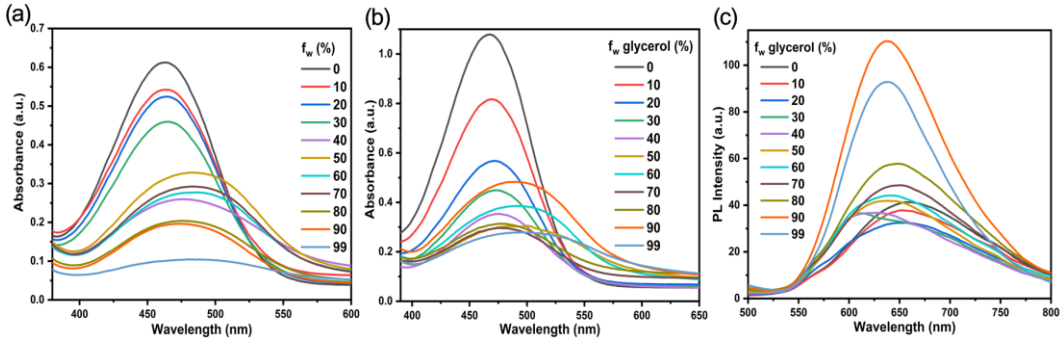

Figure S9. The absorption spectra of **Y8** in different proportions of water and DMSO (a). The absorption (b) and emission spectra (c) of **Y8** in different proportions of glycerol and ethanol.

9. Mechanochromic behavior of Y8.

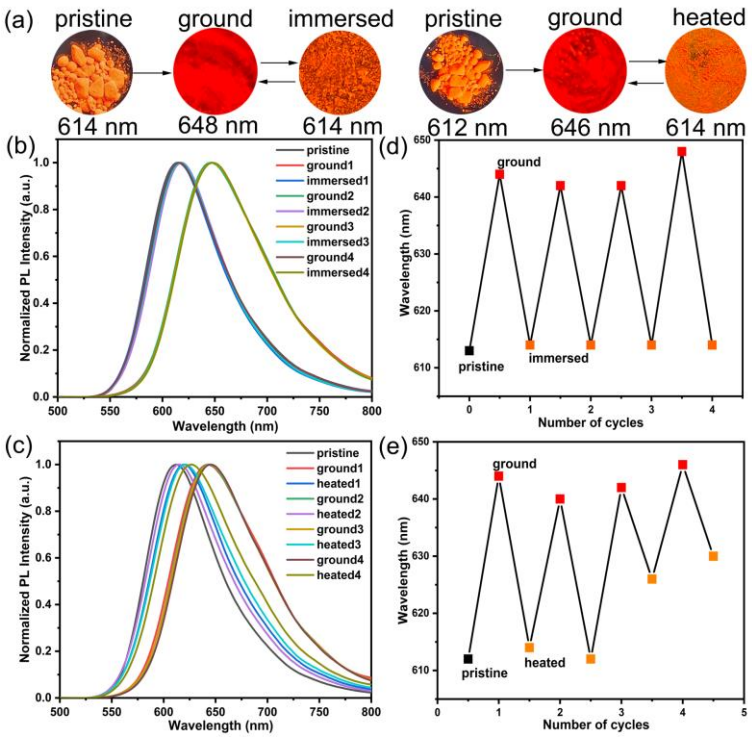

Figure S10. (a) The photographs of **Y8** taken under a 365 nm hand-held UV lamp at different states. Normalized PL spectra of **Y8** at ground-immersed (b) and ground-heated process (c). The process of ground-immersed treatment (d) and ground-heated treatment (e) with 4 cycles.

10. The XRD and DSC analyses of Y8.

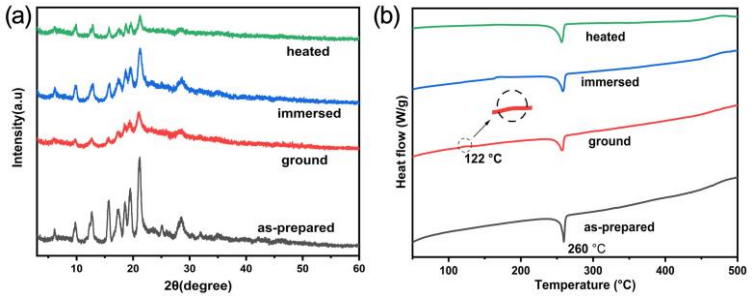

Figure S11. (a) Powder X-ray diffraction patterns of **Y8** in different states: pristine (black line), ground (red line), immersing with acetone (blue line) and heating (green line). (b) DSC curves of **Y8** in different states at room temperature.

11. Application of Y8 at 365 UV light.

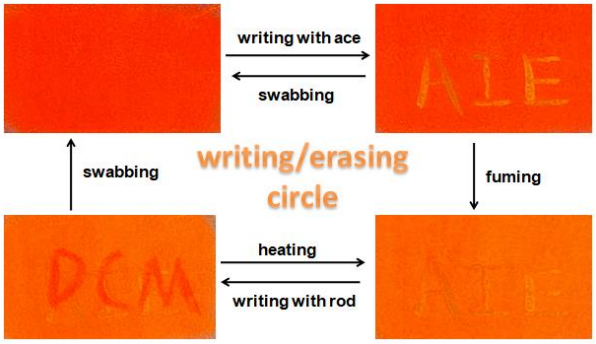

Figure S12. Photographs of weighing papers rewriting and erasing circle with **Y8** at 365uv light.

12. The spectra of Y7 and Y8 in acid condition.

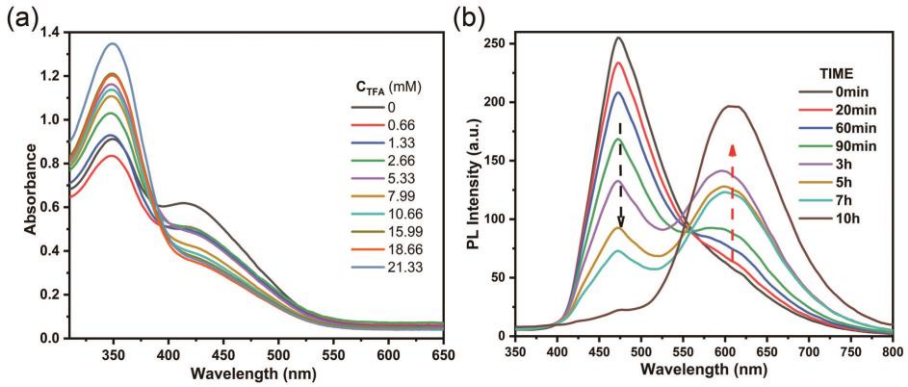

Figure S13. (a) The absorption spectra of **Y7** with different concentration (0.66 – 21.33 mM) of TFA in the respective solutions of MeOH. (b) The emission spectra of **Y8** coated on filter paper.

13. Crystal date of Y6 and Y7.

Crystal-structure of BTD-Se-TPE was gained on a Bruker APEX DUO CCD system by means of single crystal X-ray diffraction experiments. The crystal was mounted on a glass fiber for diffraction experiment. Intensity data were collected on a Nonius Kappa CCD diffractometer with Mo Kα radiation (0.71073 Å) at room temperature. The structure was solved by a combination of direct methods (SHELXS-97) and Fourier difference techniques and refined by full-matrix least-squares (SHELXL-97). All non-hydrogen atoms were refined anisotropically. Crystallographic data in this paper have been deposited in the Cambridge Crystallographic Data Centre as supplemental publication CCDC 2068421 (**Y6**), 2107708 (**Y7**).

Table S4. Crystal data and structure refinement parameters of **Y6.**

Identification code	**Y6**
Empirical formula	$C_{29}H_{24}N_2O_3$
Formula weight	448.50
Temperature/K	149.98
Crystal system	triclinic
Space group	P-1

a/Å	8.5109(4)
b/Å	10.9100(6)
c/Å	13.3920(7)
α/°	72.423(2)
β/°	80.480(2)
γ/°	80.481(2)
Volume/Å3	1160.27(10)
Z	2
ρcalcg/cm3	1.284
μ/mm-1	0.084
F(000)	472.0
Radiation	MoKα (λ=0.71073)
2Θ range for data collection/°	5.512 to 55.064
Index ranges	-11 ≤ h ≤ 11, -14 ≤ k ≤ 14, -17 ≤ l ≤ 17
Reflections collected	33125
Independent reflections	5320 [Rint = 0.0510, Rsigma = 0.0325]
Data/restraints/parameters	5320/0/308
Goodness-of-fit on F2	1.031
Final R indexes [I≥2σ (I)]	R1 = 0.0437, wR2 = 0.0960
Final R indexes [all data]	R1 = 0.0607, wR2 = 0.1064
Largest diff. peak/hole/e Å-3	0.20/-0.21

Table S5. Fractional Atomic Coordinates ($\times 10^4$) and Equivalent Isotropic Displacement Parameters ($Å^2 \times 10^3$) for **Y6**. U_{eq} is defined as 1/3 of the trace of the orthogonalised U_{IJ} tensor.

Atom	*x*	*y*	*z*	U(eq)
$O^{(2)}$	6284.5(5)	6547.2(4)	5157.4(3)	28.94(11)
$O^{(3)}$	7530.2(5)	6460.6(4)	3555.9(3)	33.23(12)
$O^{(1)}$	1673.7(5)	4164.4(5)	10299.9(4)	49.57(16)
$N^{(1)}$	3202.7(6)	6216.7(5)	8798.2(3)	31.42(13)
$N^{(2)}$	7987.8(7)	-892.8(5)	10340.7(4)	42.48(16)
$C^{(13)}$	8641.2(6)	2771.9(5)	7289.6(4)	29.46(15)
$C^{(10)}$	6920.0(6)	4417.6(5)	6086.6(4)	25.63(14)
$C^{(7)}$	8455.1(6)	3544.7(5)	4580.3(4)	27.50(14)
$C^{(15)}$	7550.0(7)	1122.0(5)	8740.1(4)	28.38(14)
$C^{(20)}$	4696.2(6)	7296.0(5)	7130.2(4)	28.29(14)
$C^{(14)}$	8867.9(7)	1717.5(5)	8155.6(4)	30.57(15)
$C^{(19)}$	5390.7(6)	6022.2(5)	7020.7(4)	27.58(14)
$C^{(12)}$	7104.3(6)	3265.7(5)	7010.7(4)	26.13(14)
$C^{(8)}$	7570.5(6)	4534.1(5)	5071.7(4)	26.10(14)
$C^{(18)}$	7793.8(7)	-2.9(6)	9628.4(4)	32.47(16)
$C^{(11)}$	6119.8(6)	5674.0(5)	6160.0(4)	26.95(14)
$C^{(9)}$	7194.3(6)	5894.6(5)	4472.2(4)	27.15(14)
$C^{(4)}$	9813.8(7)	3804.4(6)	3846.0(4)	31.44(15)
$C^{(6)}$	7935.8(7)	2332.3(6)	4814.6(5)	34.16(16)
$C^{(25)}$	3615.2(7)	7375.8(6)	8044.0(4)	30.67(15)
$C^{(16)}$	6013.3(7)	1600.5(6)	8466.4(5)	34.25(16)
$C^{(26)}$	2178.6(7)	5466.1(6)	8481.8(5)	34.58(17)
$C^{(3)}$	10615.1(7)	2878.6(6)	3362.6(4)	35.13(17)

Atom	*x*	*y*	*z*	U(eq)
$C^{(17)}$	5792.6(7)	2672.9(6)	7608.9(4)	32.75(16)
$C^{(2)}$	10077.0(7)	1683.3(6)	3578.7(4)	35.67(16)
$C^{(24)}$	3045.0(7)	8594.9(6)	8184.8(5)	38.09(17)
$C^{(21)}$	5142.6(7)	8442.0(6)	6404.0(4)	32.97(16)
$C^{(5)}$	8737.5(7)	1422.2(6)	4318.0(5)	38.42(17)
$C^{(23)}$	3508.2(8)	9712.5(6)	7457.3(5)	40.86(18)
$C^{(22)}$	4560.7(7)	9641.0(6)	6560.4(5)	38.04(17)
$C^{(29)}$	2577.6(8)	6287.4(7)	9869.7(5)	42.78(19)
$C^{(28)}$	2590.0(8)	4937.5(8)	10605.3(5)	49.1(2)
$C^{(27)}$	2219.9(8)	4127.1(7)	9247.3(5)	45.1(2)
$C^{(1)}$	10891.7(9)	725.4(7)	2992.2(5)	49.6(2)

Table S6. Crystal data and structure refinement parameters of **Y7.**

Identification code	**Y7**
Empirical formula	$C_{29}H_{24}N_2O_2$
Formula weight	432.50
Temperature/K	300.3
Crystal system	triclinic
Space group	P-1
a/Å	8.5715(12)
b/Å	10.3297(14)
c/Å	14.4352(19)
α/°	108.324(4)
β/°	103.699(5)
γ/°	98.925(4)
Volume/Å^3	1141.7(3)
Z	2
ρ_{calc}g/cm^3	1.258
μ/mm^{-1}	0.079
F(000)	456.0
Radiation	MoKα (λ=0.71073)
2Θ range for data collection/°	5.05 to 54.992
Index ranges	$-11 \le h \le 11$, $-13 \le k \le 13$, $-18 \le l \le 18$
Reflections collected	38470
Independent reflections	5241 [R_{int} = 0.1508, R_{sigma} = 0.0902]
Data/restraints/parameters	5241/0/299
Goodness-of-fit on F^2	1.008
Final R indexes [I>=2σ (I)]	R_1 = 0.0714, wR_2 = 0.1360
Final R indexes [all data]	R_1 = 0.1695, wR_2 = 0.1807
Largest diff. peak/hole/e Å^{-3}	0.20/-0.20

Table S7. Fractional Atomic Coordinates ($\times 10^4$) and Equivalent Isotropic Displacement Parameters ($Å^2 \times 10^3$) for **Y7**. U_{eq} is defined as 1/3 of the trace of the orthogonalised U_{IJ} tensor.

Atom	*x*	*y*	*z*	U(eq)
$O^{(1)}$	3059.2(11)	5254.9(9)	3720.9(5)	65.6(3)
$O^{(2)}$	4005.8(10)	6906.6(8)	5305.8(5)	52.7(3)
$N^{(1)}$	6660.8(11)	10011.8(9)	9086.2(6)	49.9(3)
$N^{(2)}$	1773.8(16)	4381.8(12)	10355.7(8)	85.4(4)
$C^{(1)}$	7447.6(17)	10228.6(14)	10805.2(9)	72.6(5)
$C^{(2)}$	7334.2(16)	11076.2(13)	10123.9(8)	61.7(5)
$C^{(3)}$	6485.2(14)	10461.7(11)	8251.9(8)	48.3(4)
$C^{(4)}$	5511.2(14)	9525.6(11)	7258.3(8)	49.5(4)
$C^{(5)}$	4577.3(13)	8139.5(11)	7108.8(8)	47.4(4)
$C^{(6)}$	3885.7(13)	6988.0(11)	6263.3(7)	46.1(4)
$C^{(7)}$	2937.2(13)	5638.9(11)	6160.1(7)	43.3(3)
$C^{(8)}$	2460.8(12)	4759.0(11)	5166.6(7)	41.8(3)
$C^{(9)}$	1467.5(13)	3295.6(11)	4658.4(7)	44.0(4)
$C^{(10)}$	1710.4(14)	2387.5(12)	3792.4(8)	54.8(4)
$C^{(11)}$	758.3(15)	1010.4(13)	3312.9(9)	59.2(4)
$C^{(12)}$	-465.8(15)	486.9(12)	3666.1(8)	55.5(4)
$C^{(13)}$	-1511.9(19)	-1007.4(13)	3117.3(10)	79.3(6)
$C^{(14)}$	7715(2)	8856.9(15)	10162.9(9)	84.7(6)
$C^{(15)}$	7184.8(17)	11847.9(13)	8386.1(9)	65.9(5)
$C^{(16)}$	6990.2(18)	12293.6(14)	7575.8(10)	74.7(5)

$C^{(17)}$	6121.6(18)	11384.8(14)	6603.3(9)	74.2(5)
$C^{(18)}$	5393.7(17)	10009.7(13)	6447.9(9)	64.7(5)
$C^{(19)}$	2660.8(13)	5357.6(11)	7063.0(7)	42.0(3)
$C^{(20)}$	3769.5(15)	4791.6(12)	7589.9(8)	53.4(4)
$C^{(21)}$	3529.5(15)	4532.7(12)	8434.5(8)	57.5(4)
$C^{(22)}$	2193.7(14)	4841.0(11)	8756.7(7)	49.1(4)
$C^{(23)}$	1079.2(15)	5403.3(12)	8237.0(8)	52.3(4)
$C^{(24)}$	1329.9(14)	5666.1(12)	7398.2(8)	49.6(4)
$C^{(25)}$	1955.9(16)	4582.9(12)	9647.1(8)	60.7(4)
$C^{(26)}$	3143.8(14)	5564.3(12)	4608.6(8)	49.4(4)
$C^{(27)}$	-709.0(16)	1395.4(13)	4525.6(8)	58.9(4)
$C^{(28)}$	231.8(14)	2768.5(12)	5011.6(8)	51.9(4)
$C^{(29)}$	7446.6(18)	8857.3(13)	9112.1(9)	76.0(5)

14. Cell Viability Assay.

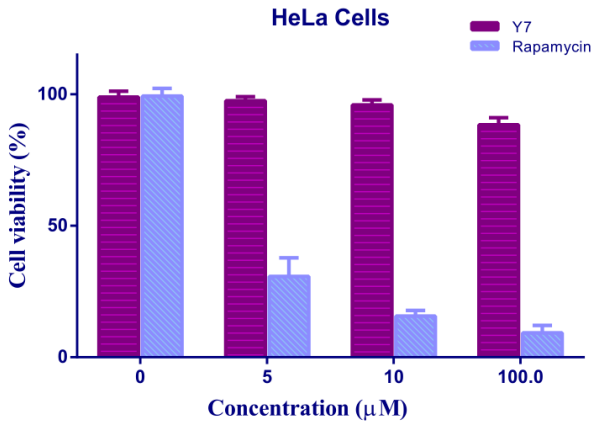

Figure S14. Cell viability values (%) estimated by MTT assays using A549 cells, cultured in the presence of 0-100.0 μM of **Y7** and Rapamycin for 24 h at 37 °C.

15. The spectra of NMR and MS.

15.1 NMR spectra of Y.

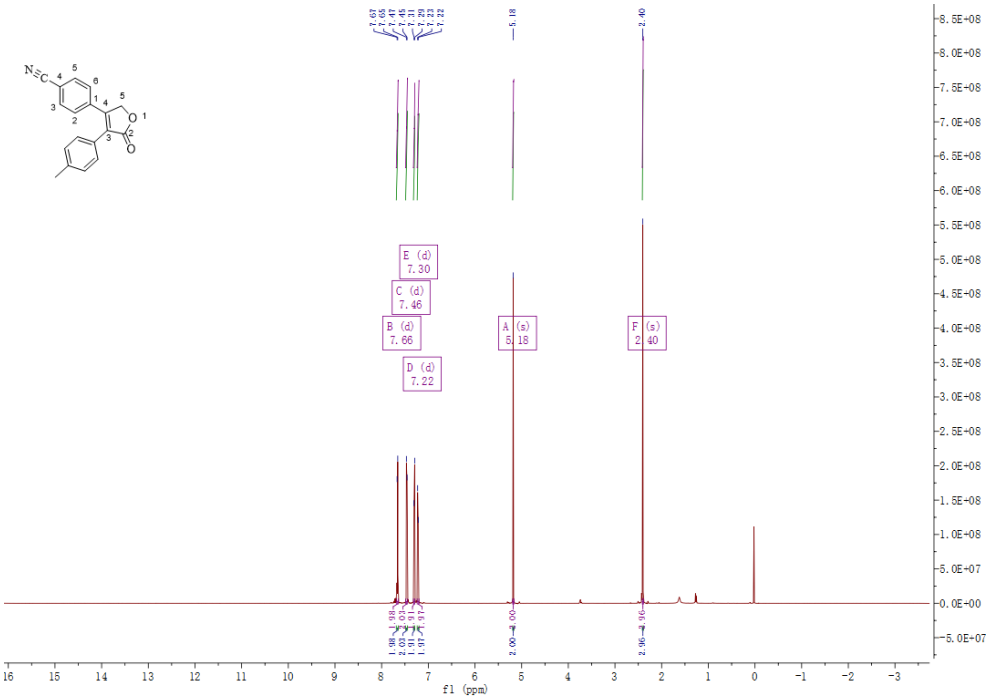

Figure S15. ^{1}H-NMR spectrum of **Y** recorded in $CDCl_3$ (600 MHz, 298K).

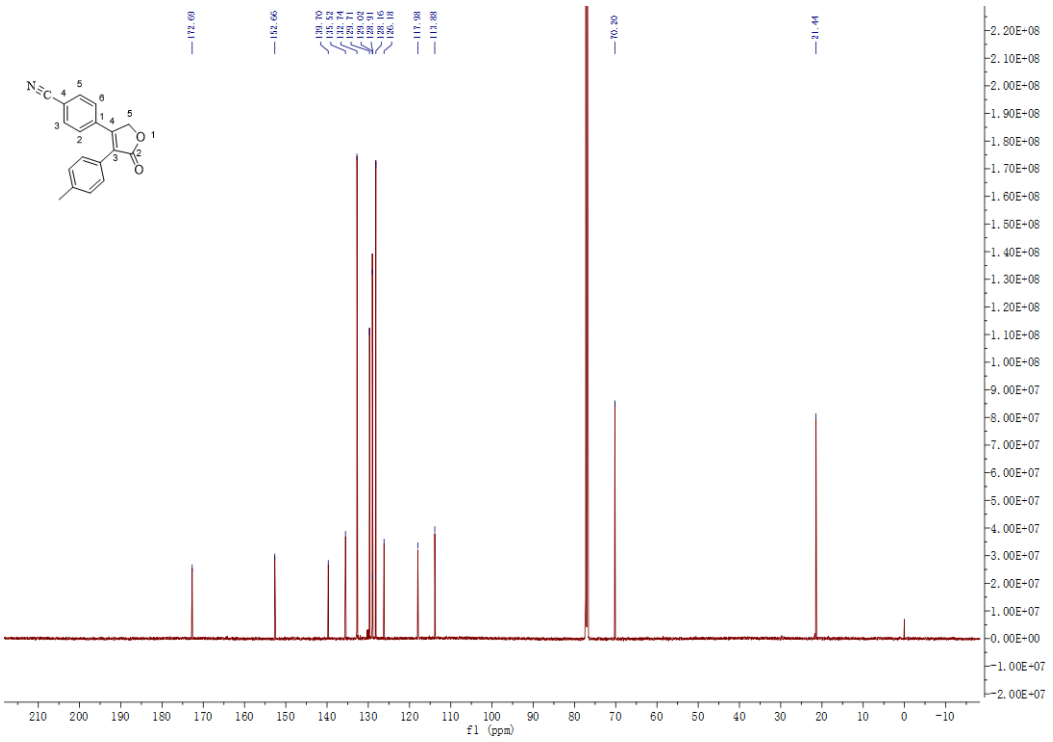

Figure S16. ^{13}C-NMR spectrum of **Y** in $CDCl_3$ (151 MHz, 298K).

15.2 NMR spectra of Y1.

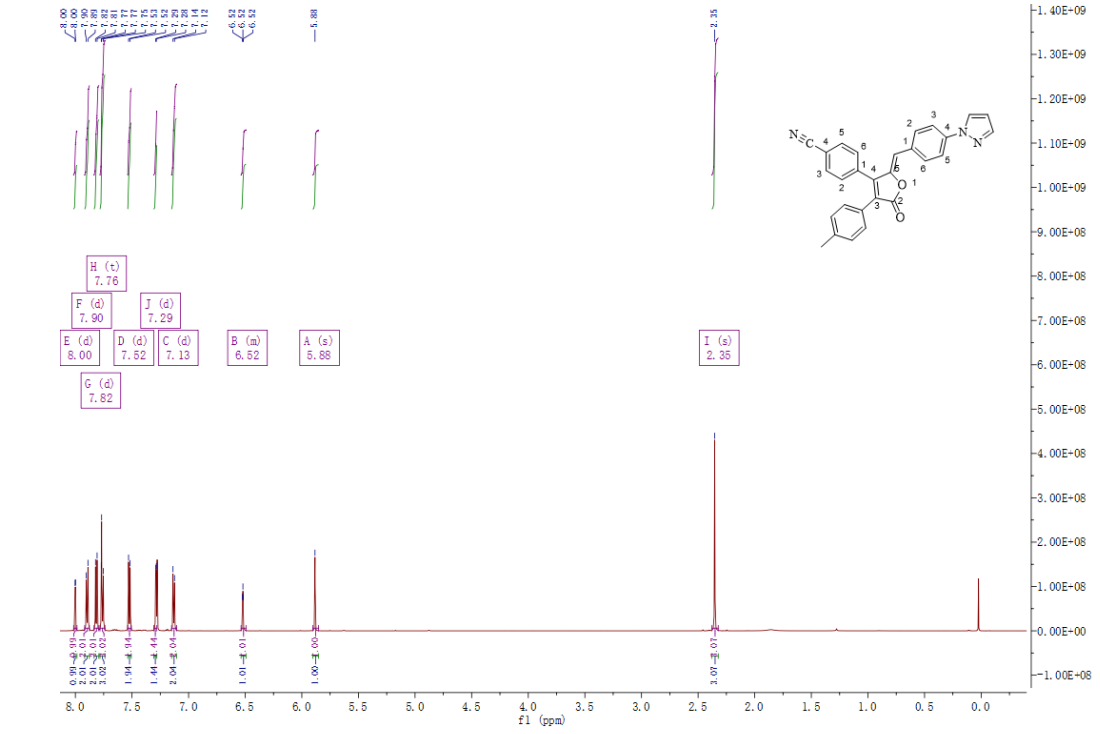

Figure S17. ^{1}H-NMR spectrum of **Y1** recorded in $CDCl_3$ (600 MHz, 298K).

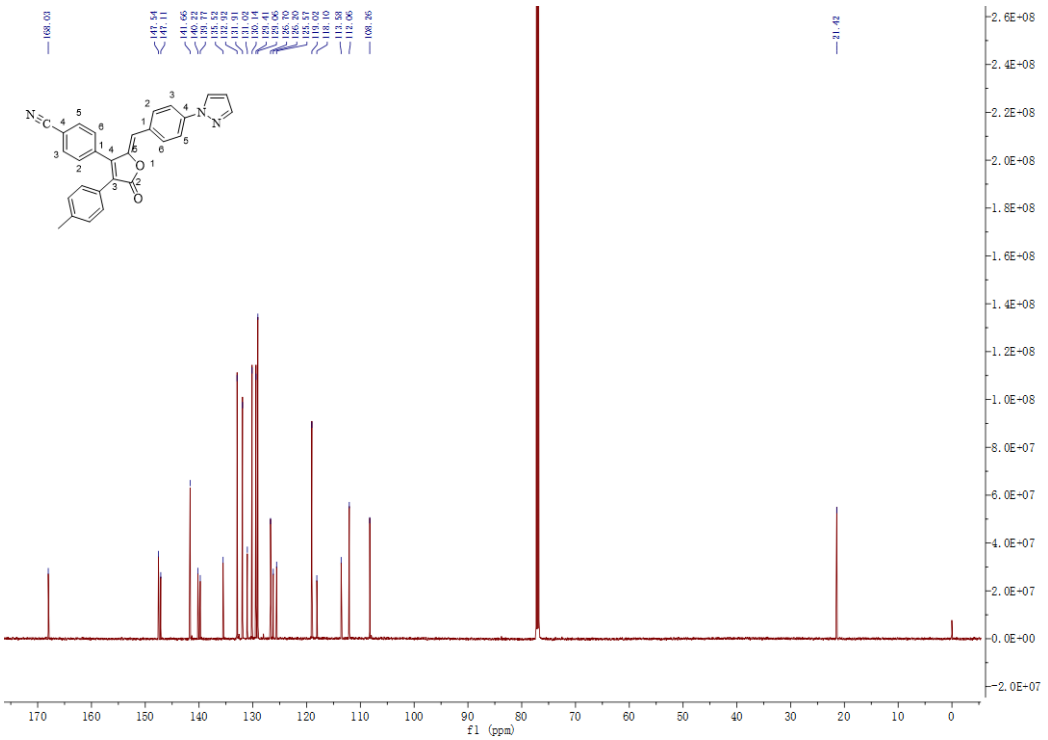

Figure S18. ^{13}C-NMR spectrum of **Y1** in $CDCl_3$ (151 MHz, 298K).

15.3 NMR spectra of Y2.

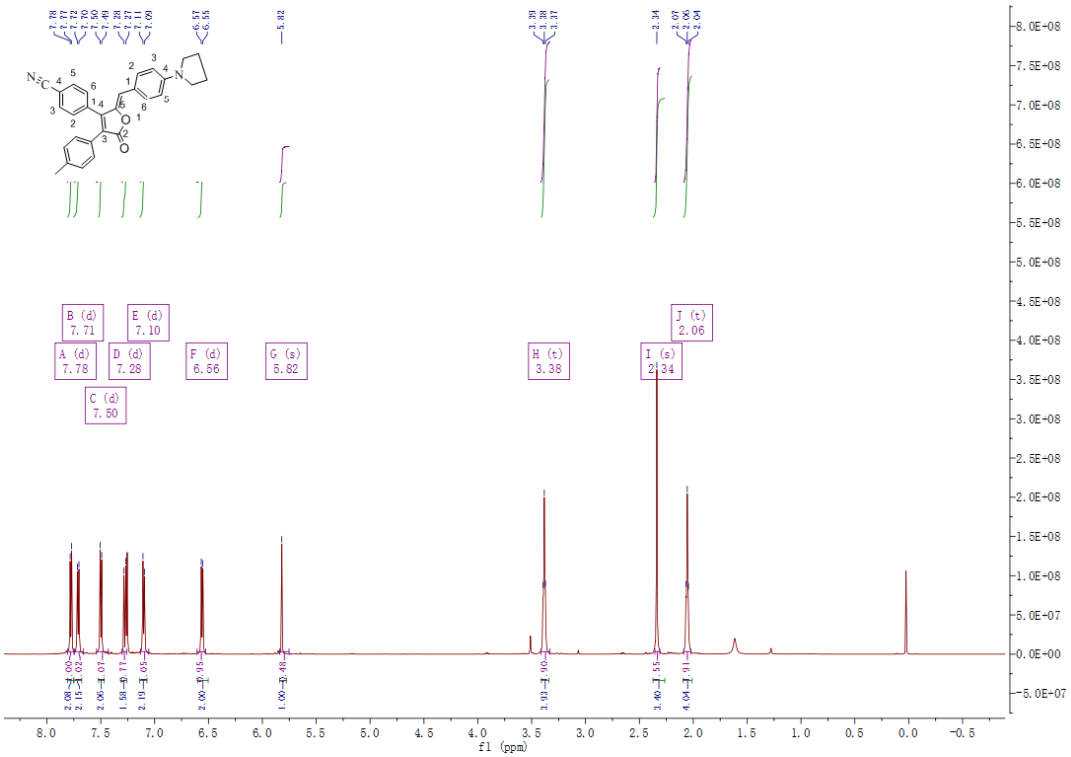

Figure S19. ^{1}H-NMR spectrum of **Y2** recorded in $CDCl_3$ (600 MHz, 298K).

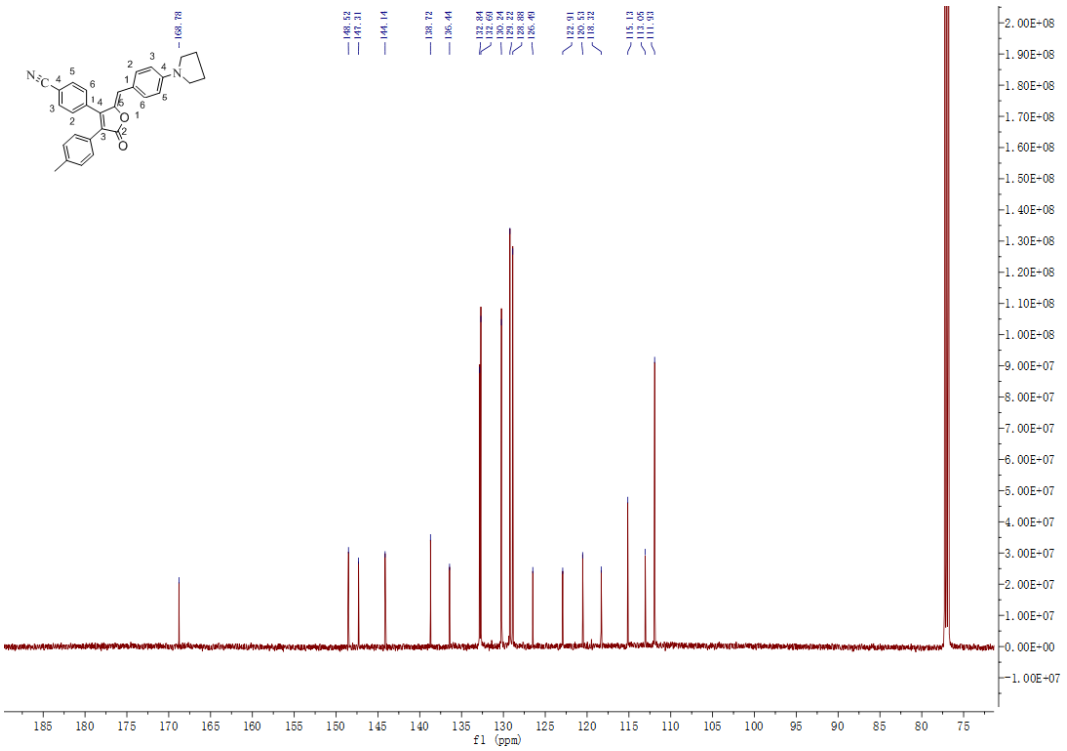

Figure S20. ^{13}C-NMR spectrum of **Y2** in $CDCl_3$ (151 MHz, 298K).

15.4 NMR spectra of Y3.

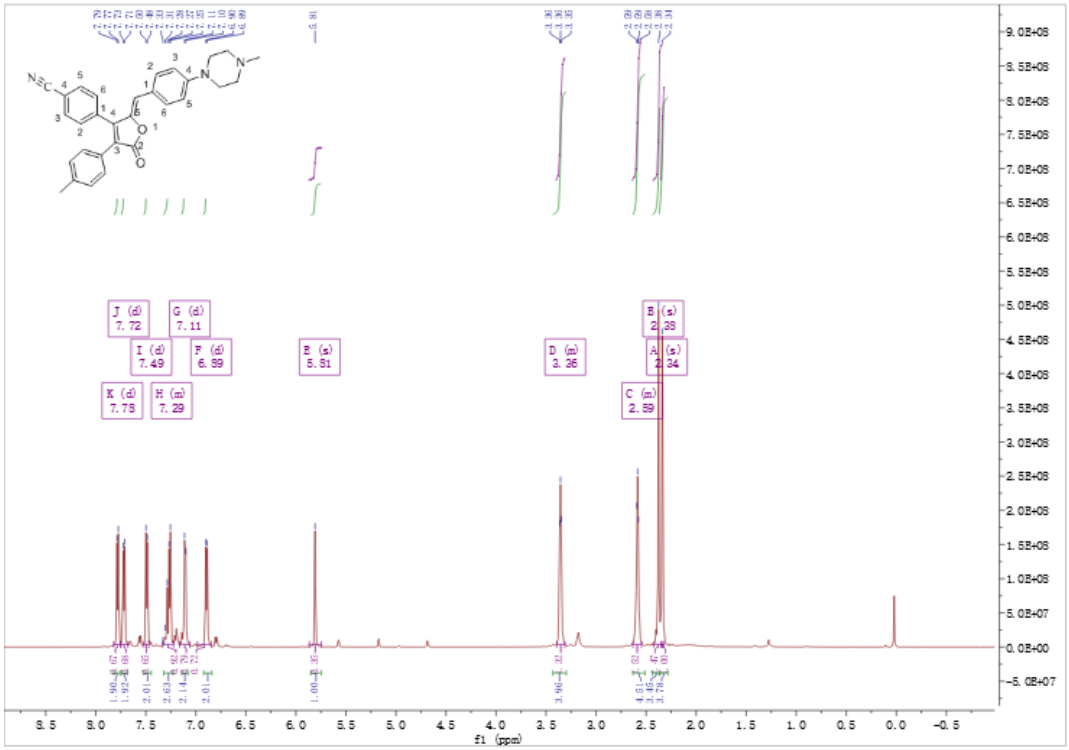

Figure S21. ^{1}H-NMR spectrum of **Y3** recorded in $CDCl_3$ (600 MHz, 298K).

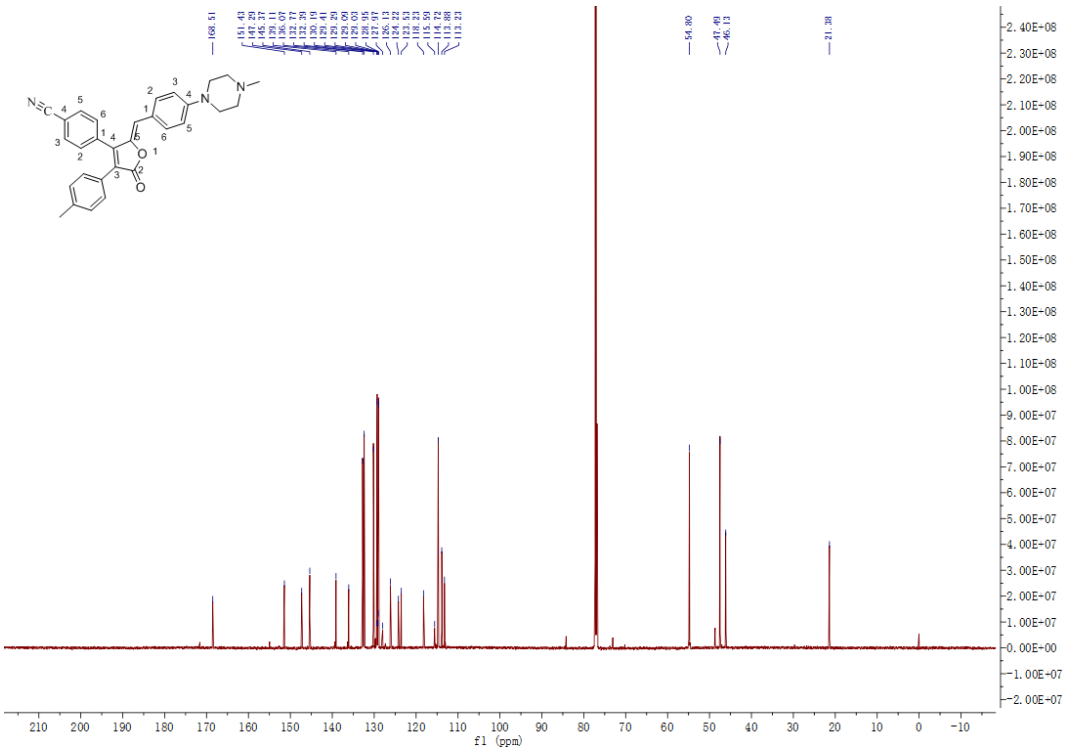

Figure S22. ^{13}C-NMR spectrum of **Y3** in $CDCl_3$ (151 MHz, 298K).

15.5 NMR spectra of Y4.

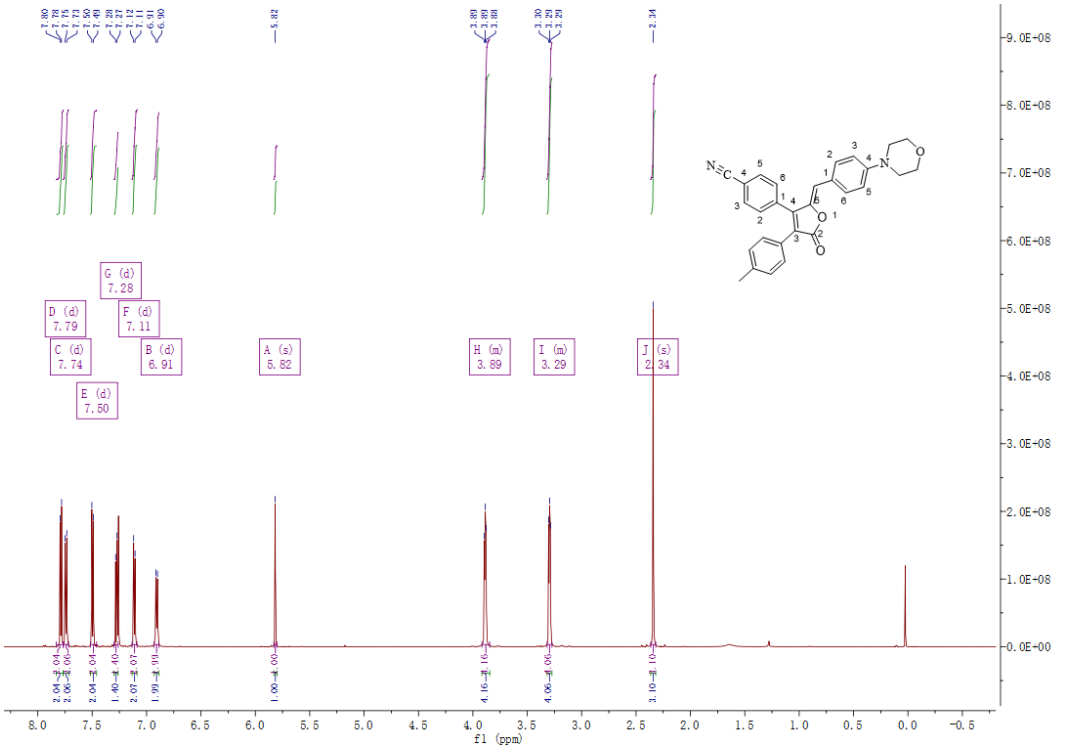

Figure S23. ^{1}H-NMR spectrum of **Y4** recorded in $CDCl_3$ (600 MHz, 298K).

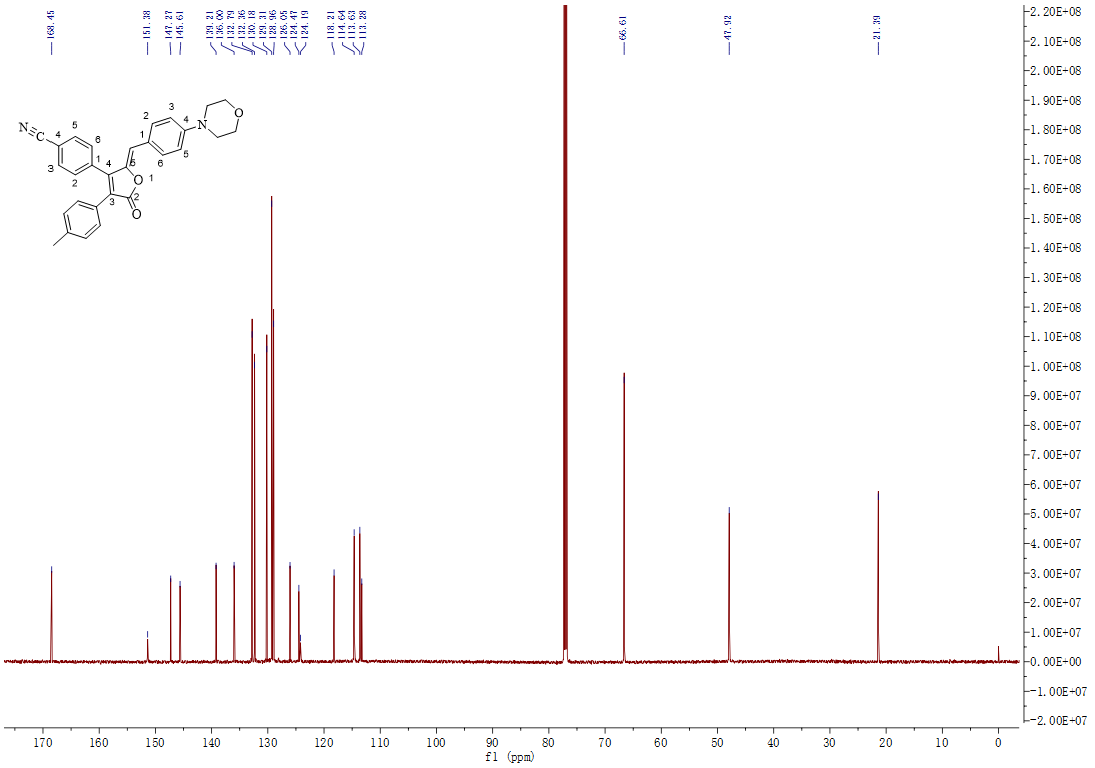

Figure S24. ^{13}C-NMR spectrum of **Y4** in $CDCl_3$ (151 MHz, 298K).

15.6 NMR spectra of Y5.

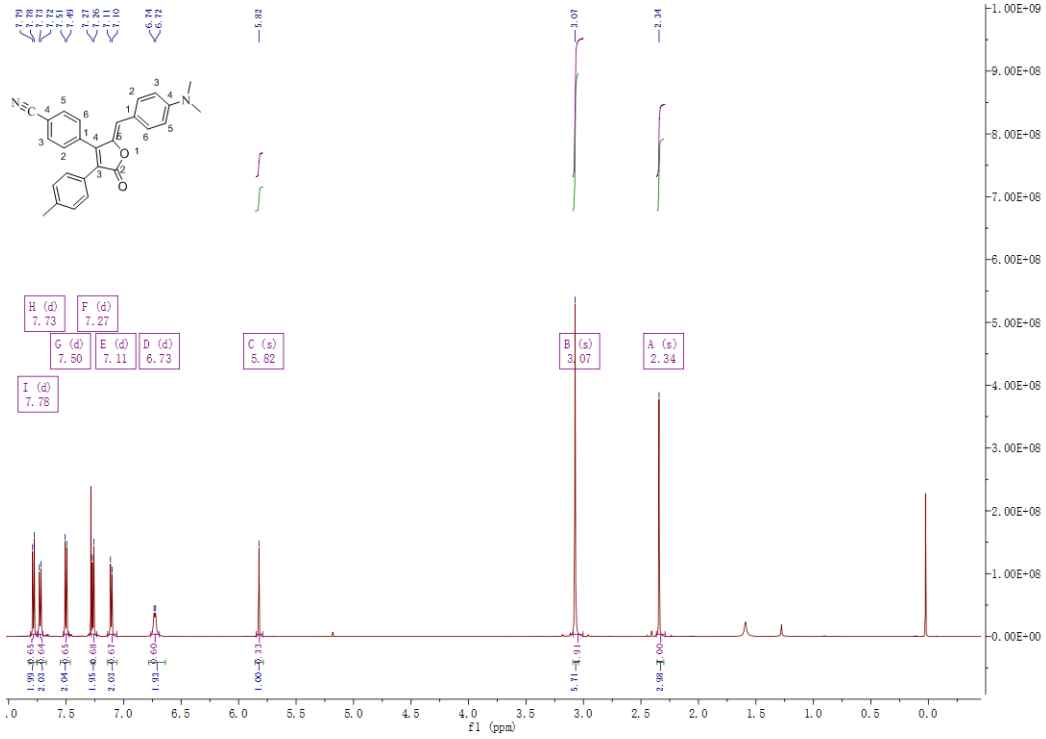

Figure S25. ^{1}H-NMR spectrum of **Y5** recorded in $CDCl_3$ (600 MHz, 298K).

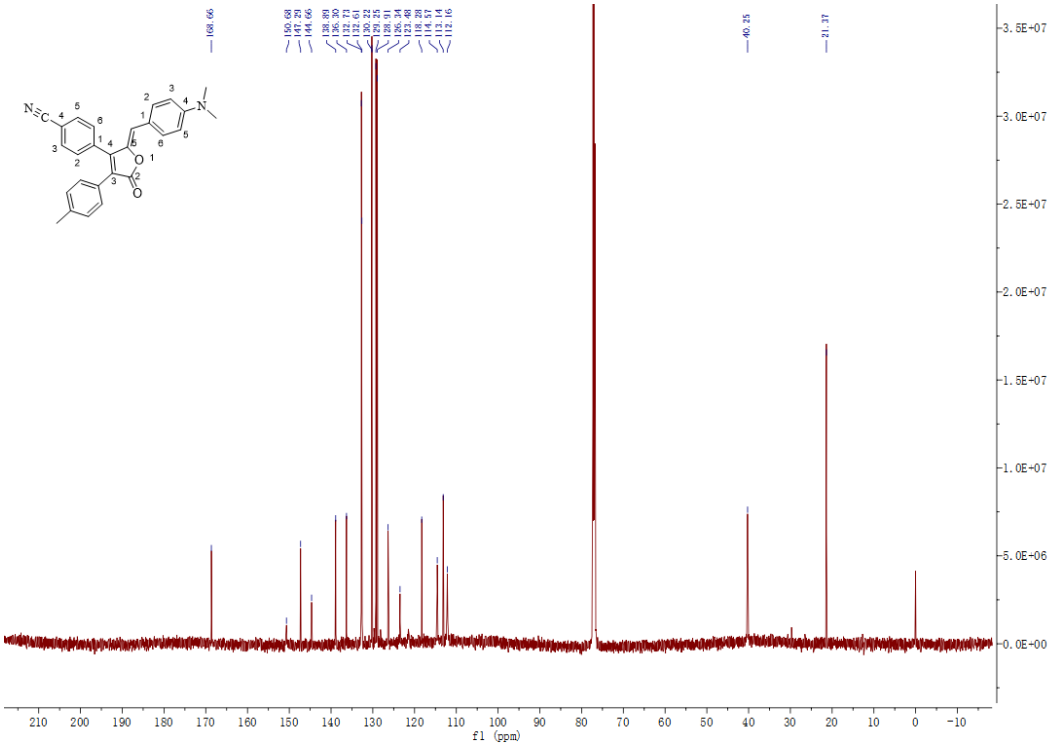

Figure S26. ^{13}C-NMR spectrum of **Y5** in $CDCl_3$ (151 MHz, 298K).

15.7 NMR spectra of Y6.

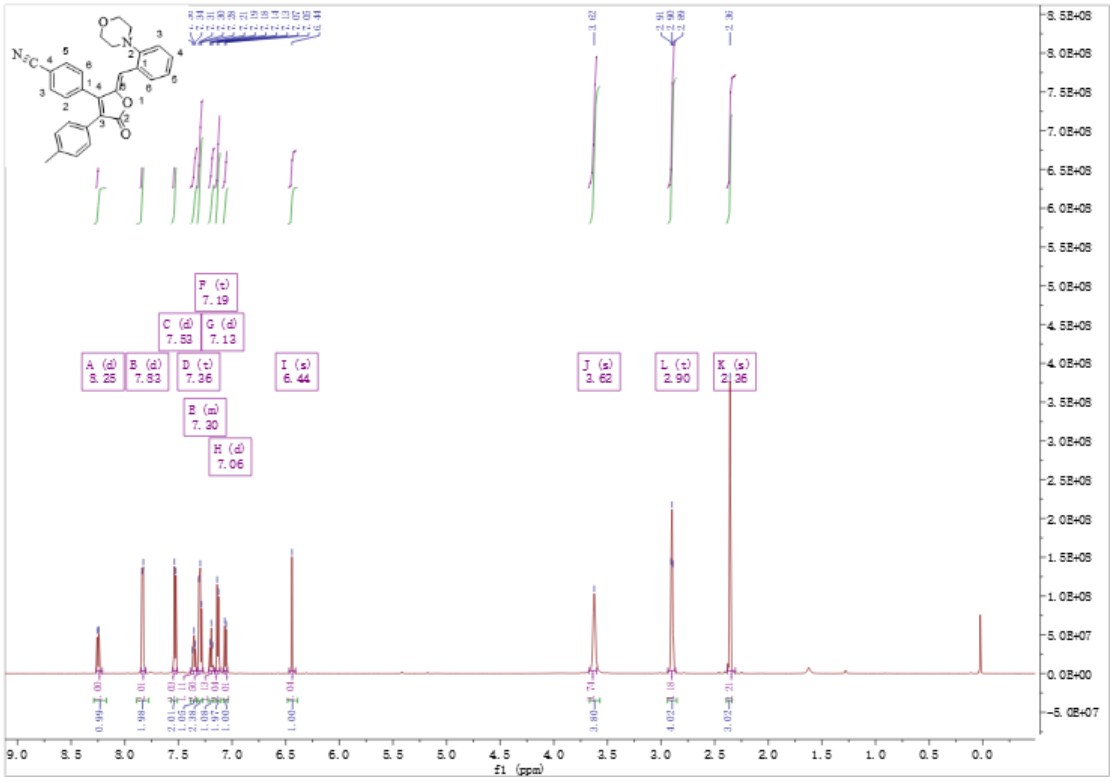

Figure S27. ^{1}H-NMR spectrum of **Y6** recorded in $CDCl_3$ (600 MHz, 298K).

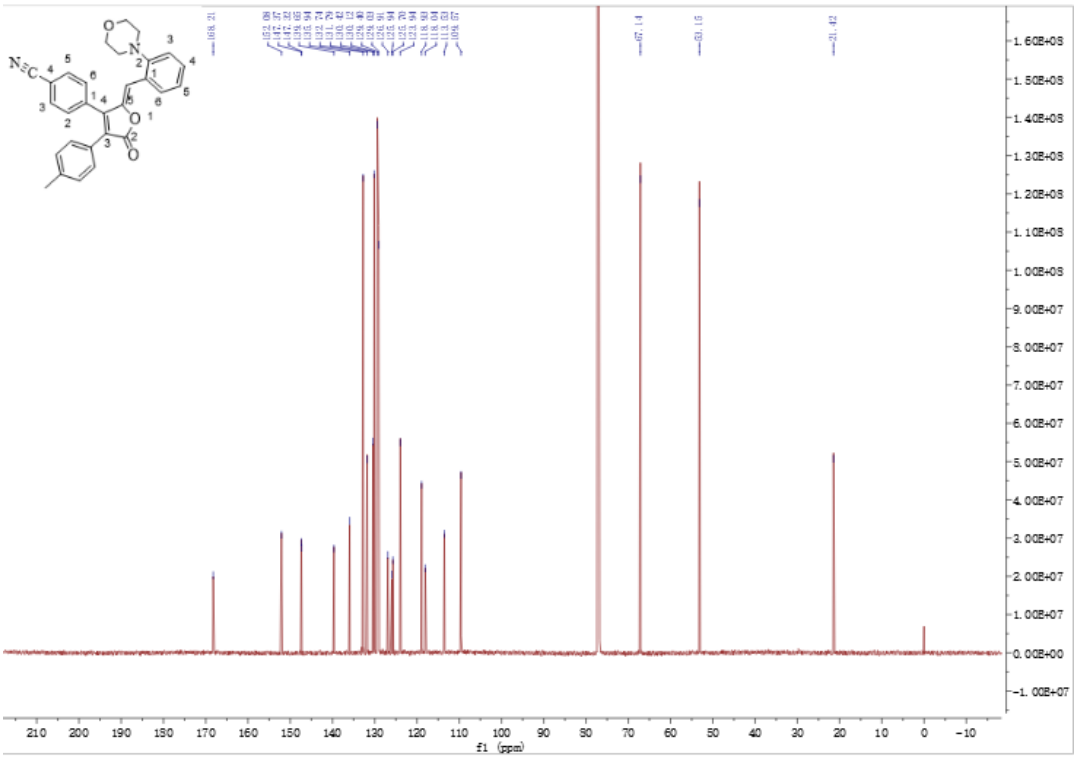

Figure S28. ^{13}C-NMR spectrum of **Y6** in $CDCl_3$ (151 MHz, 298K).

15.8 NMR spectra of Y7.

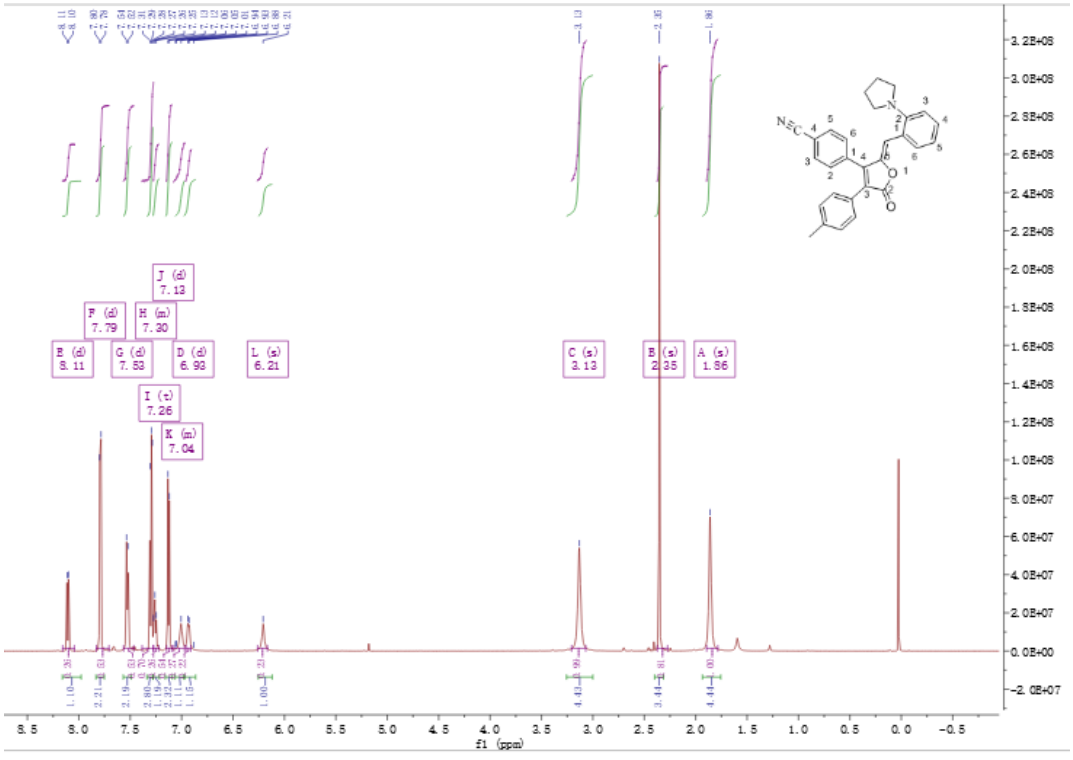

Figure S29. ^{1}H-NMR spectrum of **Y7** in $CDCl_3$ (600 MHz, 298K).

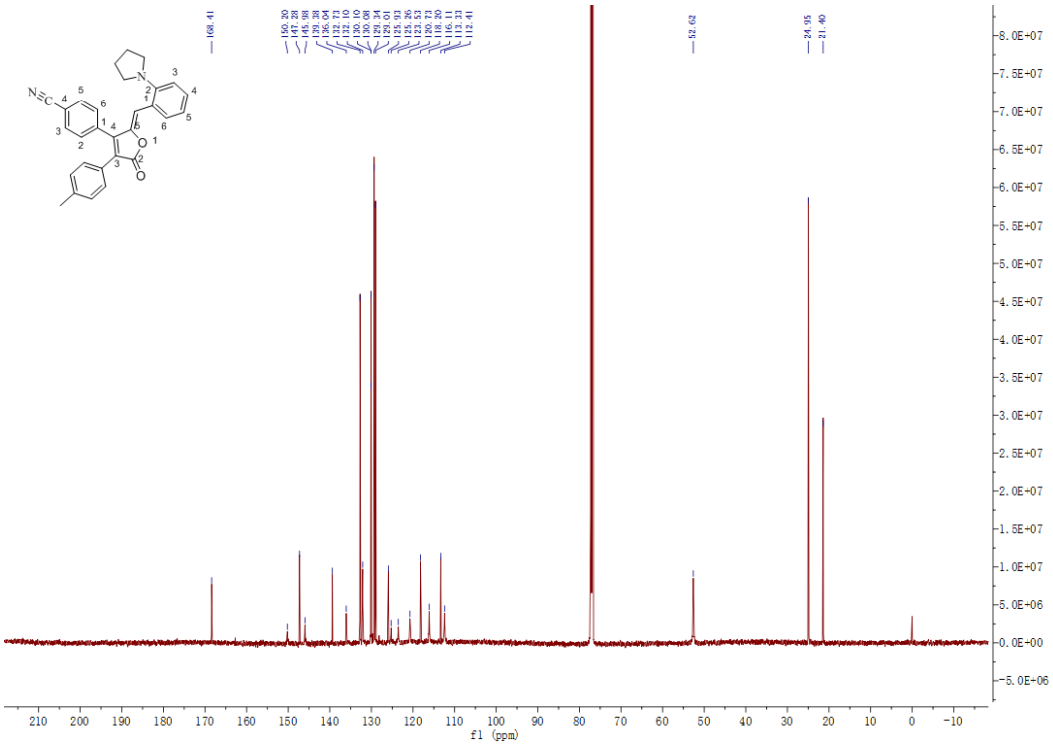

Figure S30. ^{13}C-NMR spectrum of **Y7** in $CDCl_3$ (151 MHz, 298K).

15.9 NMR spectra of Y8.

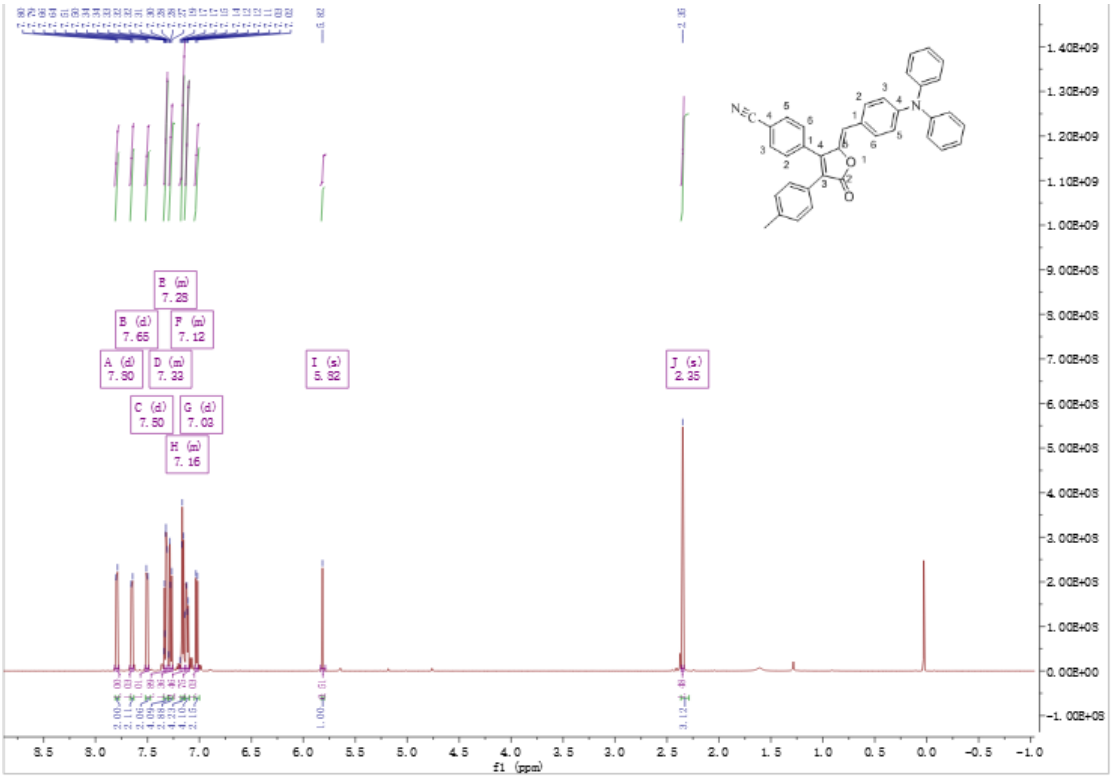

Figure S31. ^{1}H-NMR spectrum of **Y8** recorded in $CDCl_3$ (600 MHz, 298K).

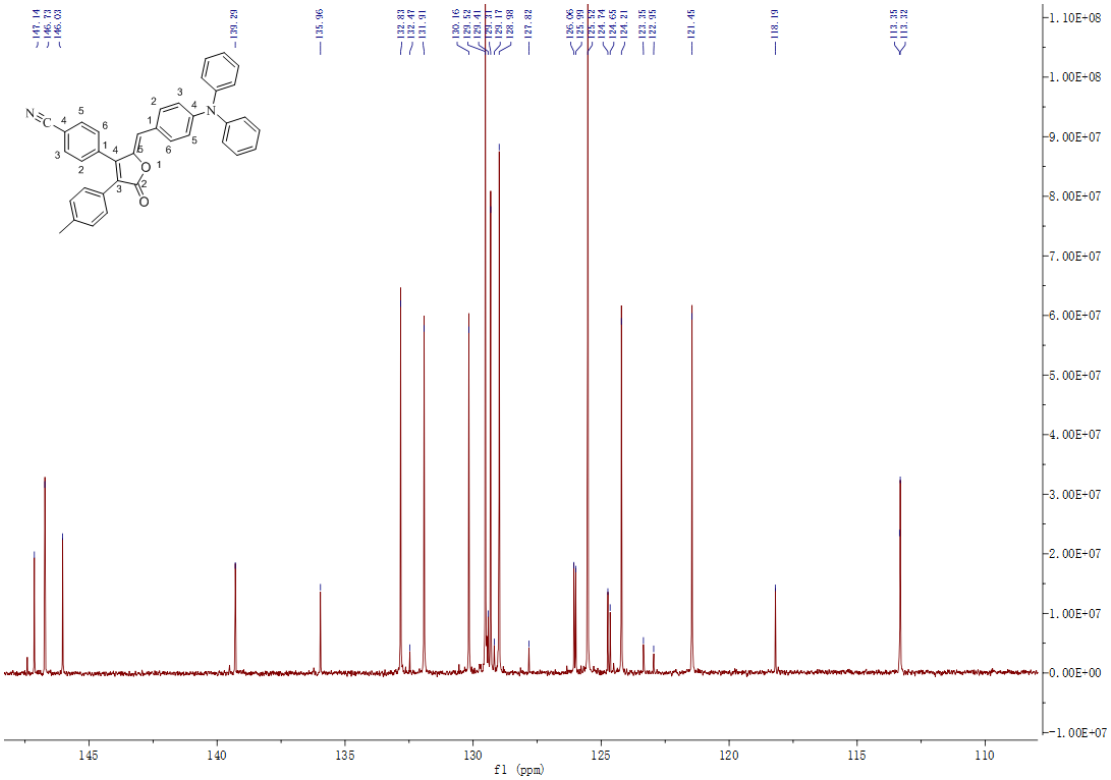

Figure S32. ^{13}C-NMR spectrum of **Y8** in $CDCl_3$ (151 MHz, 298K).

16. HRMS Spectra of Compounds.

16.1 HRMS Spectrum of Y.

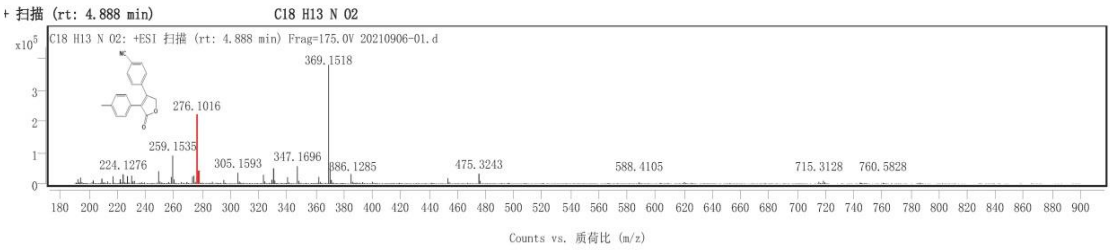

Figure S33. HRMS spectrum of **Y**.

16.2 HRMS Spectrum of Y1.

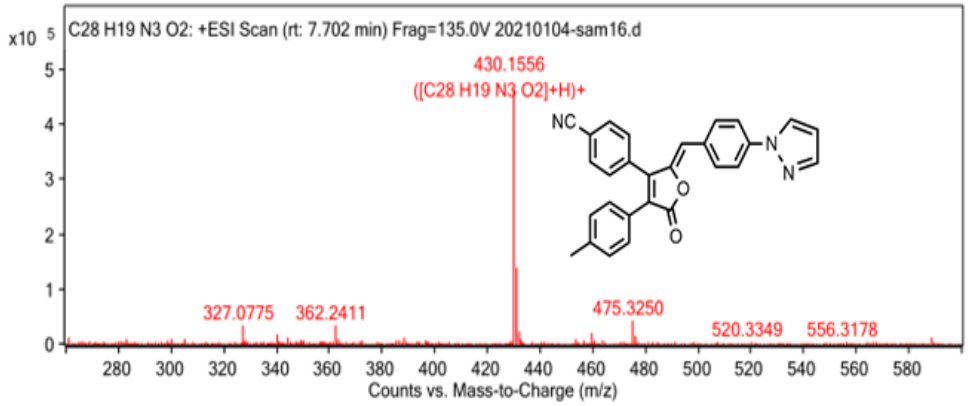

Figure S34. HRMS spectrum of **Y1**.

16.3 HRMS Spectrum of Y2.

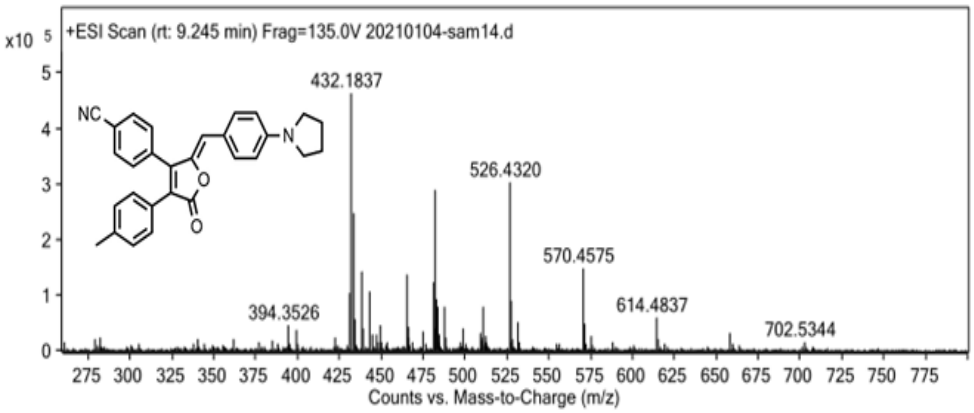

Figure S35. HRMS spectrum of **Y2**.

16.4 HRMS Spectrum of Y3.

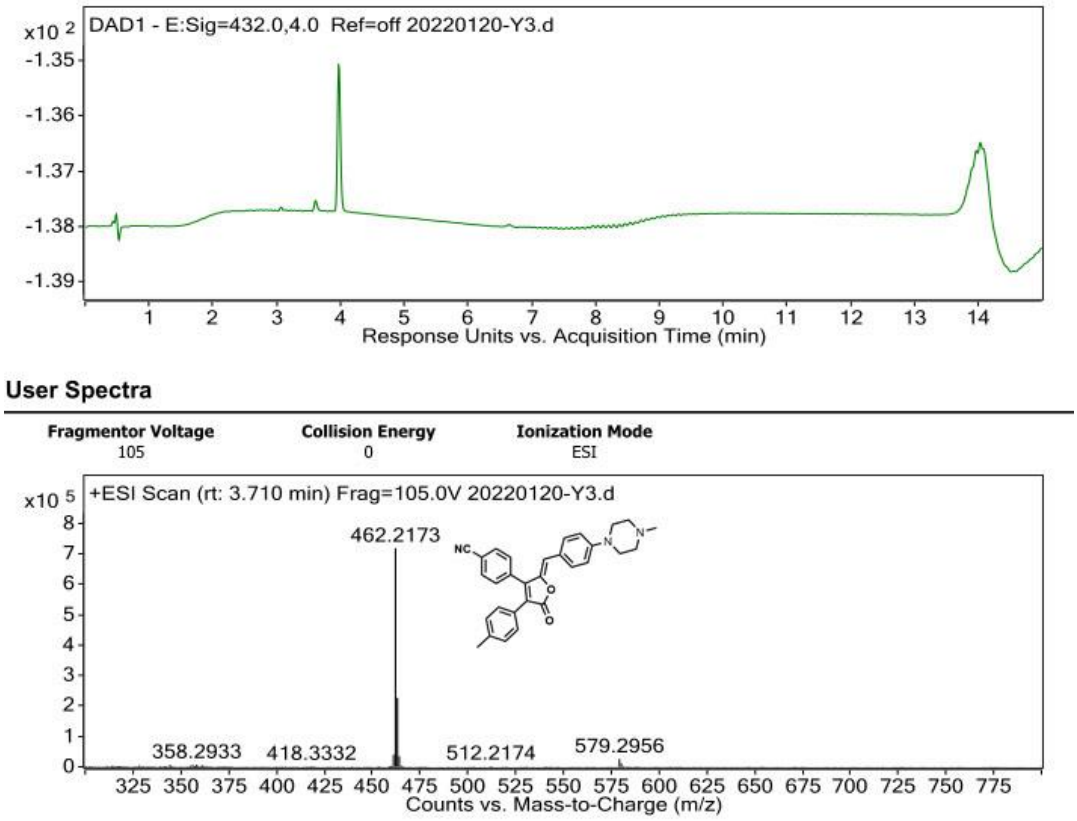

Figure S36. HRMS spectrum of **Y3**.

16.5 HRMS Spectra of Y4.

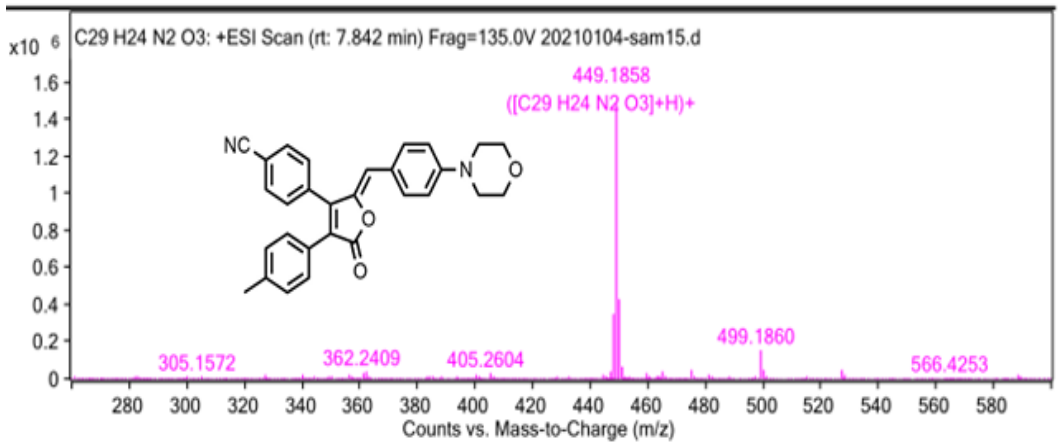

Figure S37. HRMS spectrum of **Y4**.

16.6 HRMS Spectrum of Y5.

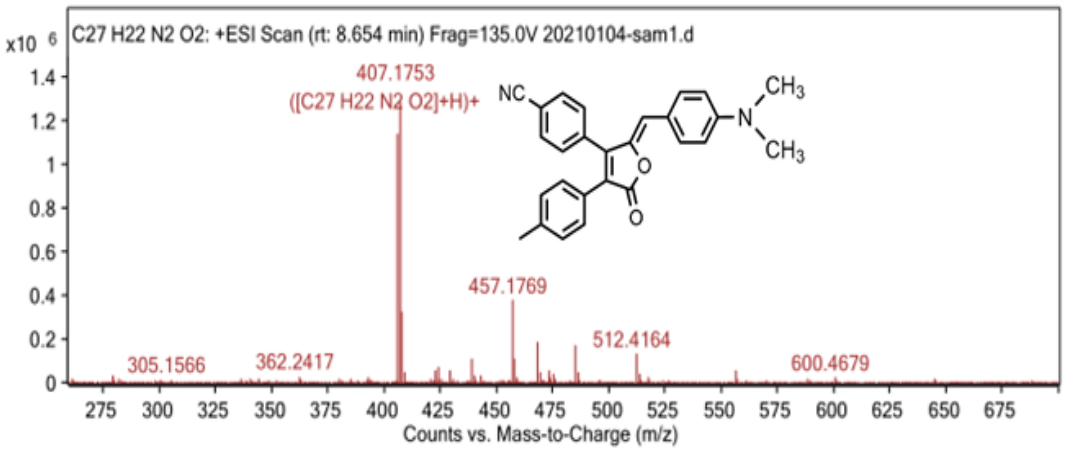

Figure S38. HRMS spectrum of **Y5**.

16.7 HRMS Spectrum of Y6.

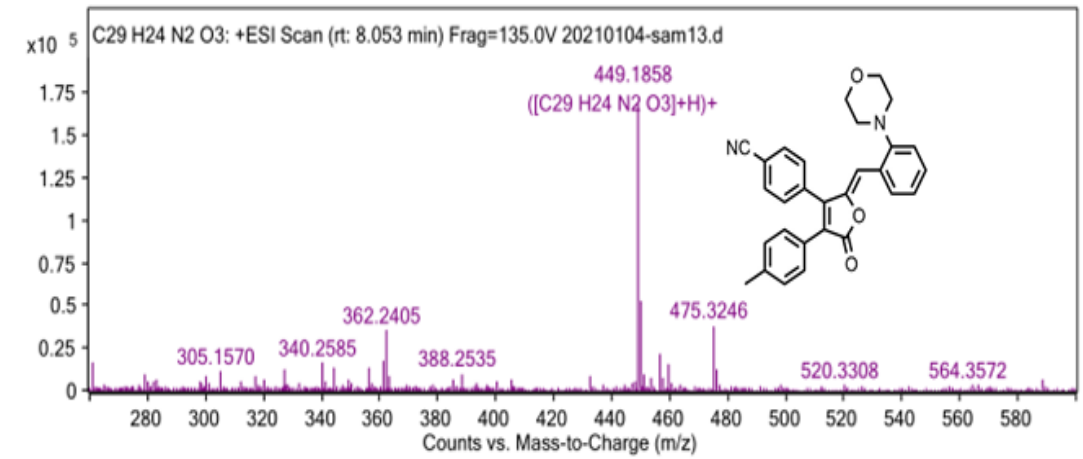

Figure S39. HRMS spectrum of **Y6**.

16.8 HRMS Spectrum of Y7.

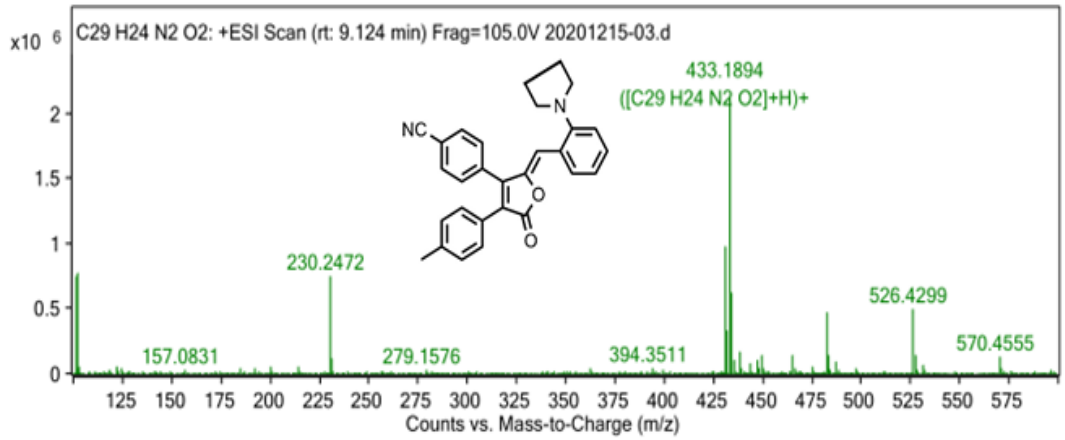

Figure S40. HRMS spectrum of **Y7**.

16.9 HRMS Spectrum of Y8.

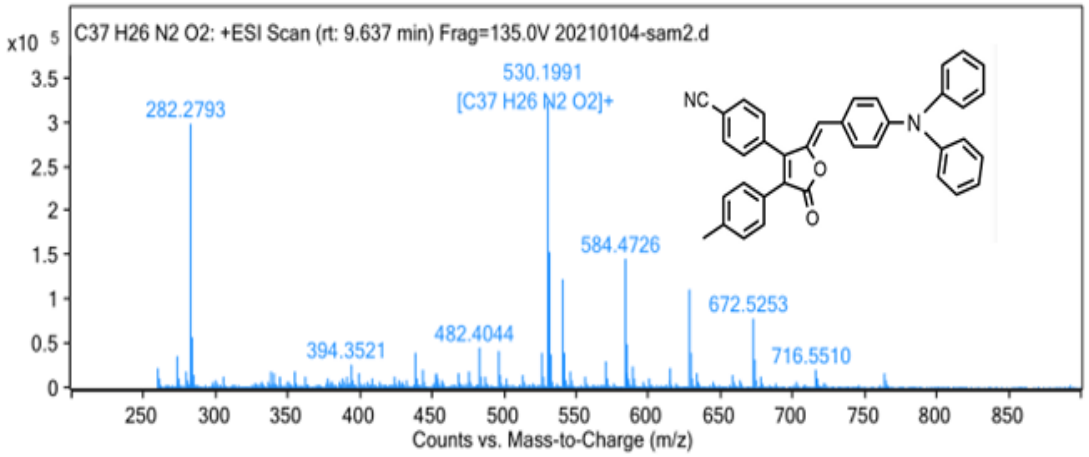

Figure S41. HRMS spectrum of **Y8**.